



Research paper

Shape identification of the jet-grouted column based on the thermal analysis and differential evolution

Marek Wojciechowski¹

Abstract: In the paper, an indirect method for the identification of the final shape of the freshly executed jet-grouted column is developed. The method relies on the backward analysis of the temperatures measured inside the column, along the trace of the injecting pipe. Temperature changes in the column are caused by the hydration process of the cementitious grout. 2D axisymmetric unsteady heat conduction initial-boundary value problem is solved for finding the column shape which fits best the reference temperature measurements. The model of the column is solved using the finite element method. The search is performed using the global evolutionary optimization algorithm called differential evolution. It is shown that the proposed method can provide an accurate prediction of the column shape if only the model reflects the physical reality well. The advantage over previous results is that the cylindrical shape of the column does not have to be assumed anymore, and the full profile of the column along its length can be accurately identified.

Keywords: jet-grouted column, transient heat transfer, cement hydration, inverse problem, differential evolution

¹PhD., Eng., Lodz University of Technology, Faculty of Civil Engineering, Architecture and Environmental Engineering, Al. Politechniki 6, 90-924 Łódź, Poland, e-mail: mwojc@p.lodz.pl, ORCID: 0000-0003-3766-2801

1. Introduction

Jet grouting is a soil improvement technique used worldwide, with increasing importance since its inception 50 years ago. The jet grouting is based on the high-pressure injection of one or more fluids (grout, air, water) into the subsoil. The fluids are injected through small-diameter nozzles placed on a pipe that, in most applications, is first drilled into the soil and is then rotated and raised towards the ground surface during jetting. The injected water-cement-soil grout cures underground, eventually producing a body made of cemented soil [1, 2].

The treated volume in the injection operation has a quasi-cylindrical shape. Many methods allowing prediction of the diameter of the jet-grouted columns have been developed, which try to take into account the physical conditions during the column execution, such as the soil type and strength, nozzle sizes, inject pressure, and others. Both the mechanistic models of the process and the data-driven models using machine learning methods are used in this context [3–6, 20]. However, the execution of the jet-grouted column with the predetermined diameter is merely impossible. This is because of the uncertainties inscribed into the soil properties and the jet injection technology. Thus, one of the important aspects of the quality control of the grouted columns is the verification of their final geometry. This is a challenging problem since direct measurements, requiring excavation of the column, are rarely possible and indirect methods have to be developed. Examples of such indirect techniques being in use are the inspection holes [1], hydraulic calipers [7], sonic logging tests [8], and the measurements and back analysis of the temperatures inside the column [9]. This last technique is especially interesting because the temperature measurements inside the column are reported to be simple and cheap to be performed. On the other hand, the strong and reliable theory related to the process of heat generation and conduction in the surrounding of the grouted area is necessary for geometry identification. The back analysis of the temperature evolution in the column has been successfully used in identifying the diameter of the cylindrically shaped columns [9]. The 1D axisymmetric heat conduction problem, at the middle cross-section of the column, is solved during the diameter identification process. A description of the commercial incarnation of this method, called TempJet, can be found in the reference [10].

This paper is an attempt to take a step forward in the topic of back analysis of temperature evolution in the jet-grouted column. The motivation is as follows. Since it is observed that the shape of the jet-grouted columns is often far from the cylindrical one (see for example Fig. 1a)), then it is reasonable to drop this assumption. As a consequence, the 2D axisymmetric heat conduction problem has to be solved during identification, to discover the shape of the column, now variable along its length. The existing measurement methods can still be exploited to obtain information about the temperatures along the column axis. Thus, enriched column shape information can be obtained at the cost of increased, but still reasonable, numerical effort. In the following sections, the identification problem at hand is formulated, then the 2D axisymmetric heat conduction initial-boundary value problem (I-BVP) is introduced and the solution details by the finite element method (FEM) are given. Finally, an example of shape identification, performed using differential evolution (DE) optimization method is provided and discussed.

2. Formulation of the identification problem

Let us suppose that some quantity u , characterizing a certain process \mathcal{R} , has been measured at chosen time moments t_k , where $k = 1, \dots, n$, and at several observed points x_j , where $j = 1, \dots, m$. The array of values $u_{kj}^{\mathcal{R}}$ has been then collected as a result of the measurements. Let us suppose also that a “direct” numerical model $\mathcal{M}(p_i)$ of this process has been built, which depends on a set of parameters p_i with $i = 1, \dots, l$, and allows to calculate $u_{kj}^{\mathcal{M}}$ – the theoretical values of u at the observed times and points. Identification of parameters p_i is recognized as an “inverse” problem. It consists in finding such a set of parameters, that the theoretical solution $u_{kj}^{\mathcal{M}}$ at the observed points is as close as possible to the measured values $u_{kj}^{\mathcal{R}}$. The following minimization problem is then solved:

$$(2.1) \quad \min_{p_i} \left[\sum_{k=1}^n \sum_{j=1}^m \left(u_{kj}^{\mathcal{M}}(p_i) - u_{kj}^{\mathcal{R}} \right)^2 \right]$$

For the case of shape identification of the jet grouted column the following interpretation of the quantities present in the above description is considered. \mathcal{R} is the process of grout curing, during which heat is generated due to the cement hydration phenomena. The measured quantity is the temperature T at the centre of the column, at times t_k and at depths z_j , i.e. $u_{kj}^{\mathcal{R}} \equiv T_{kj}^{\mathcal{R}} = T^{\mathcal{R}}(z_j, t_k)$. The spatial resolution of measurements equal to 0.3 m is technologically possible [10]. Model \mathcal{M} is an axisymmetric initial-boundary value problem (I-BVP) formulated for unsteady heat transfer inside the column and its surroundings, solved by means of the finite element method (FEM). Using this model, the theoretical temperatures at the corresponding times and locations are computed: $u_{kj}^{\mathcal{M}} \equiv T_{kj}^{\mathcal{M}} = T^{\mathcal{M}}(z_j, t_k)$. Model \mathcal{M} , and especially the temperature distribution at the center line of the column, depend on many parameters, such as: injection composition (cement hydration heat curve, w/c ratio), heat transfer coefficients of soil and soil-concrete mixture, initial temperature of the soil, external air temperature, surface heat exchange coefficient and other. All these quantities are possible to be established using the data gathered during column design and execution. What is an unknown here, necessary to be identified, is the diameter of the column along its length. Diameter variations strongly influence the amount of heat generated during concrete maturing and the temperature distribution observed in column. Thus, the column diameters at the same depths as temperature measurements ($i = j$), are taken as the model parameters, i.e.: $p_j = D_j = D(z_j)$. The minimization problem Eq. (2.1) can be then rewritten as follows:

$$(2.2) \quad \min_{D_j} \left[\sum_{k=1}^n \sum_{j=1}^m \left(T_{kj}^{\mathcal{M}}(D_j) - T_{kj}^{\mathcal{R}} \right)^2 \right]$$

Solving problem Eq. (2.2) leads to the set of optimal diameters denoted as D_j^{opt} . Assuming that other aspects of the numerical model are fitting well the physical reality, it can be also assumed that this solution approximates well the real shape of the column, i.e., $D_j^{\text{opt}} \approx D_j^{\mathcal{R}}$, where $D_j^{\mathcal{R}}$ are the real column diameters.

It should be noted that the optimization problem Eq. (2.2) must be solved using the global optimization methods since the gradient of the minimized function simply cannot be given. The differential evolution (DE) algorithm is adopted for this purpose (see Section 4.2).

3. I-BVP for heat transfer

3.1. Geometry of the problem

A vertical jet-grouted column of the length L executed from the ground surface has been considered. The cross-section of the column, which is irregular in general, is assumed to possess a circular shape with the centre located at the trace of the injecting pipe (z axis in Fig. 1b, 1c). Possible irregularities and eccentricities in cross-section shape are not considered in this paper. The diameter of the cross-section can still vary along the depth, i.e., $D = D(z)$, thus the side boundary of the column is seen as a surface of the revolution created by rotating the column edge around the z axis. The geometry of the column can be then reduced to the 2D axisymmetric problem. In addition, if it is assumed that also thermal properties of the soil and the grouted column are independent of the circumferential direction, the BVP considered here becomes an axisymmetric unsteady heat transfer problem.

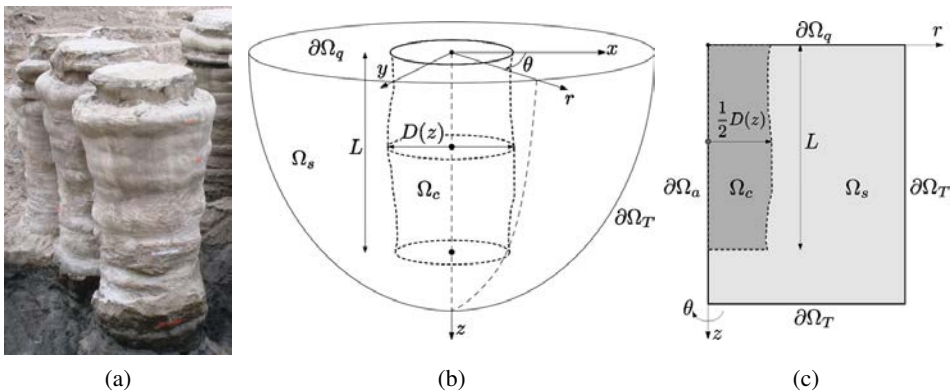


Fig. 1. (a) Example of the excavated jet-grouted column; (b) model of the column immersed in 3D half-space of the soil; (c) 2D representation of the axisymmetric geometry; (source: <https://www.undergroundconsulting.it>)

It should be stressed, that this geometry is chosen for reflecting the most common case. However, the identification method presented in this paper is general enough to cover also other cases, specifically the diagonal or horizontal jet-grouted columns.

3.2. Heat transfer equations

The governing equations for the transient heat conduction, in their strong form, along with the boundary and initial conditions, can be expressed as follows:

$$(3.1) \quad \rho c_p \dot{T} = -q_{i,i} + h \quad \text{on } \Omega = \Omega_s + \Omega_c$$

$$(3.2) \quad q_i = -kT_{,i} \quad \text{on } \Omega = \Omega_s + \Omega_c$$

$$(3.3) \quad h = \begin{cases} 0 & \text{on } \Omega_s \\ h_c & \text{on } \Omega_c \end{cases}$$

$$(3.4) \quad q_i n_i = \begin{cases} 0 & \text{on } \partial\Omega_a \\ \kappa(T - T_\infty) & \text{on } \partial\Omega_q \end{cases}$$

$$(3.5) \quad T = T_0 \quad \text{on } \partial\Omega_T$$

$$(3.6) \quad t = 0: T = T_0 \quad \text{on } \Omega$$

In the above equations, ρ is the material density, c_p is the specific heat capacity, k is the isotropic heat conduction coefficient, T is the temperature, q_i is the heat flux vector, h is the volumetric heat source, caused here by the chemical reactions related to the cement hydration process and n_i is the unitary vector normal to the boundary. The time derivative of temperature is denoted as \dot{T} . Spatial derivatives are denoted by commas in index notation. For the external surface, the heat exchange coefficient κ and the external (air) temperature T_∞ are introduced. Surface radiation is omitted in this formulation. In the case of the axisymmetric problem, at the axis of rotational symmetry, i.e., at $\partial\Omega_a$, the natural, zero outward flux boundary condition is defined. Initially, at time $t = 0$, the temperature distribution T_0 is assumed at the whole domain. At later times temperature is kept constant only at the boundary $\partial\Omega_T$, via the Dirichlet boundary conditions. All quantities present in Eqs. (3.1)–(3.6) are position and time dependent. The heat source term is of special importance here since it is the loading term causing heat flow and temperature evolution inside the column. Heat production is non-zero only inside the volume occupied by the column, which is denoted as h_c .

Starting from the set of Eqs. (3.1)–(3.6), the weak form of these equations for the axisymmetric problem can be derived. It is written as:

$$(3.7) \quad \int_{\Omega} r (\rho c_p \dot{T}) \bar{T} d\Omega = - \int_{\Omega} r k T_{,i} \bar{T}_{,i} d\Omega + \int_{\partial\Omega_q} r \kappa (T - T_\infty) \bar{T} d\partial\Omega + \int_{\Omega_c} r h_c \bar{T} d\Omega$$

$$(3.8) \quad t = 0: \int_{\Omega} r (\rho c_p T) \bar{T} d\Omega = \int_{\Omega} r (\rho c_p T_0) \bar{T} d\Omega$$

where $\Omega = [r \times z]$ is a 2D axisymmetric domain. The unknown temperature $T(r, z, t)$ must belong to the set of continuously differentiable functions (at least once) fulfilling essential boundary conditions Eq. (3.5), i.e.: $T(r, z, t) = T_0(r, z, t)$ at $\partial\Omega_T$. $\bar{T}(r, z)$ is an arbitrary

weighting test function also belonging to the set of continuously differentiable functions and fulfilling condition $\bar{T}(r, z) = 0$ at $\partial\Omega_T$.

3.3. Solution by finite element method

For solving Eqs. (3.7) and (3.8), the finite element method (FEM) is used. The domain is discretized into triangular elements and the functions defined on Ω are then interpolated by the polynomial shape functions described on these elements and depending on the function values at element nodes. Linear shape functions are enough for this problem. FEM formulation leads to the system of first-order time differential equations, which is written in matrix form as:

$$(3.9) \quad \mathbf{C}\dot{\mathbf{T}} = \mathbf{K}\mathbf{T} + \mathbf{f}$$

$$(3.10) \quad t = 0: \quad \mathbf{T} = \mathbf{T}_0$$

where \mathbf{T} is the global vector of searched temperatures at the nodes of the finite element mesh at times $t \geq 0$, $\dot{\mathbf{T}}$ are the time derivatives of the temperatures (also at the nodes of the mesh), \mathbf{C} is the global capacitance matrix, \mathbf{K} is the global conductivity matrix with the term resulting from convective heat exchange at the surface added, and \mathbf{f} is the load vector which results both from the presence of the heat sources and the heat exchange at the surface. All these quantities are time dependent. In the solution approach used in this paper, the full capacitance matrix was replaced by the equivalent diagonal matrix $\hat{\mathbf{C}}$ of the lumped nodal capacitances. Matrix $\hat{\mathbf{C}}$ is trivially invertible. This allows for representing Eq. (3.9) in the form of a regular system of ordinary differential equations (ODEs):

$$(3.11) \quad \dot{\mathbf{T}} = \hat{\mathbf{K}}\mathbf{T} + \hat{\mathbf{f}}$$

with $\hat{\mathbf{K}} = \hat{\mathbf{C}}^{-1}\mathbf{K}$ and $\hat{\mathbf{f}} = \hat{\mathbf{C}}^{-1}\mathbf{f}$, which can be solved by general purpose integration techniques. The initial condition Eq. (3.10) still holds. In this paper the implicit time integration, based on the backward differentiation formula (BDF), is used, with varying approximation order of the solution, as described in [11, 12] and implemented in [13]. The right-hand side of the Eq. (3.11) is a non-linear problem solved by means of the quasi-Newton approach and with the sparse direct linear solver.

The whole solution procedure of the axisymmetric heat transfer problem has been implemented in the framework of the *fempy* project [14]. The meshes used in computations were generated using the Gmsh software [15]. Additionally, for fast sparse direct solver the Umfpack library was used [16].

4. Identification example

4.1. Reference jet-grouted column

For identification example, the reference data reflecting the installation conditions, shape, and temperature distribution in the jet-grouted column has been generated numeri-

cally. The utilization of data collected from the field measurements is considered not to be the crucial point at this stage of the theoretical work.

Geometry used for obtaining reference data is shown in Fig. 2a. The column of the length 6 m and with the diameter at the ground surface equal to 1.5 m was considered. At the characteristic depths located every 0.6 m the diameter was drawn randomly from the range (0.9, 2.0) m. Resulting reference depths and diameters are then given by $z_j = [0.0, 0.6, 1.2, 1.8, 2.4, 3.0, 3.6, 4.2, 4.8, 5.4, 6.0]$ m and $D_j^{R*} = [1.500, 1.804, 0.976, 1.244, 1.256, 1.747, 1.707, 1.805, 1.153, 2.039, 1.587]$ m. Between the reference points the diameter of the column was interpolated linearly. The average diameter of the column was then equal to $D_{avg}^{R*} = 1.53$ m.

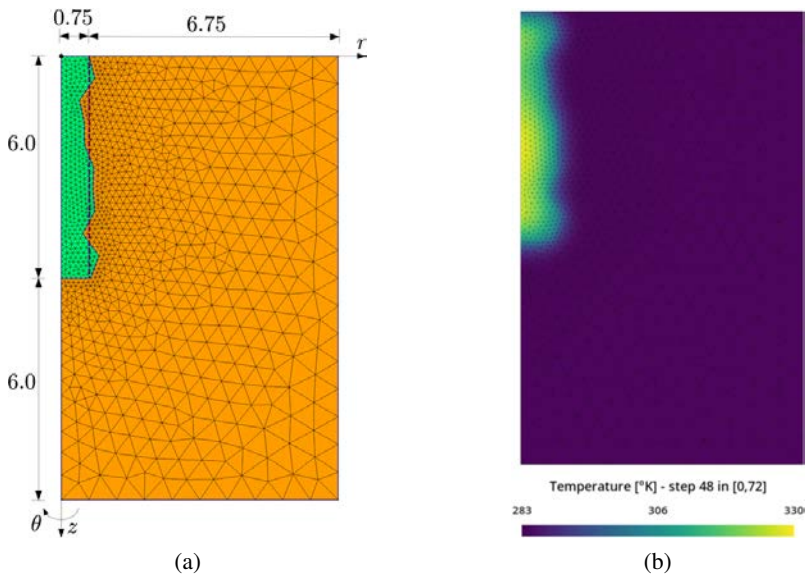


Fig. 2. Reference model of the jet-grouted column: a) dimensions and the finite element discretization; b) temperature distribution 48 hours after column execution

Table 1. Thermal parameters of the jet-grouted column and the surrounding soil

	ρ [kg/m ³]	c_p [J/(kg·K)]	k [W/(m·K)]	T_0 [K]
Column (green)	2300	900	1.8	293.15
Soil (orange)	1800	1200	0.8	283.15

Thermal parameters adopted for the grouted column and the soil body are shown in Table 1. Additionally, the heat exchange coefficient at the surface is taken as $\kappa = 8$ W/(m²·K) and the external air temperature is taken as $T_\infty = 283.15$ K. Time characteristic of the cement hydration process is presented in Fig. 3. It reflects (approximately) the amount of heat generated during the hydration of Portland cement, with the assumption that the

cement content in the grouted column is about 500 kg/m^3 . This is a very simple hydration model where there is no dependence visible between the heat production rate and the current temperature or water content – heat production depends on time only.

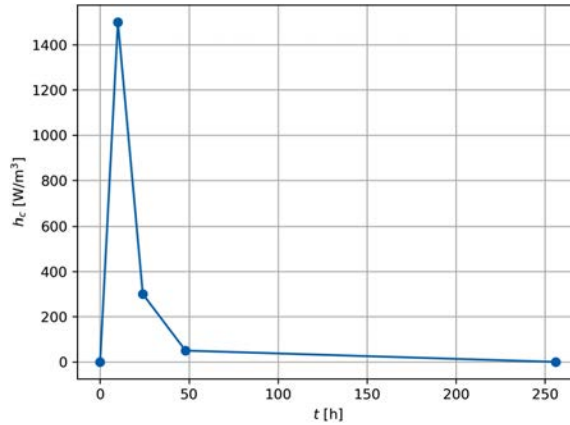


Fig. 3. Adopted heat production rate in the jet-grouted column (cement content is about 500 kg/m^3)

The reference model was solved for the time range from 0 to 72 hours. It was assumed, somewhat arbitrarily, that further computations are not relevant for shape identification. Snapshot of the temperature distribution in the whole domain after 48h is shown in Fig. 2b. For identification purposes, only the temperatures at the centre of the column are needed, at the control depths where they are supposed to be measured. In Fig. 4 the temperature evolution at the axis of symmetry is then shown with the results plotted using 4-hour time step.

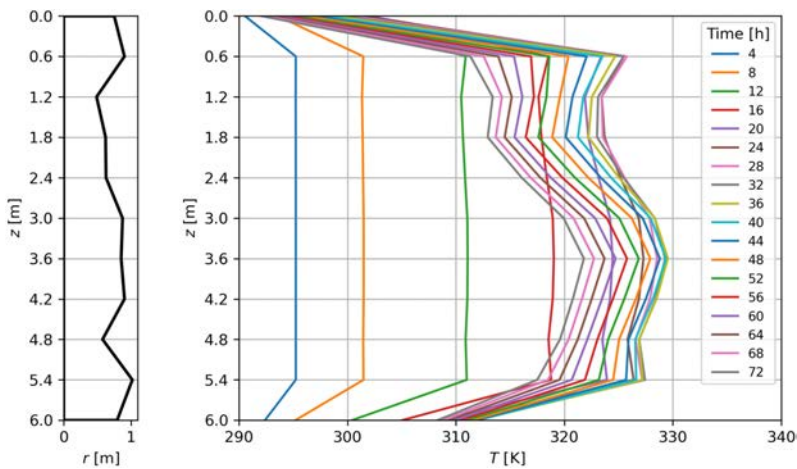


Fig. 4. On the left: the shape of the reference column; on the right: temperature evolution at the column axis. The results are plotted for the 18 time moments t_k and for 11 depths z_j

It is visible that at the beginning the temperature inside the column rises almost uniformly (except at the column ends, where the increase is slower, because of the heat outflow), and after circa 24 hours the cooling of the column begins and then also the uniformity of the temperature distribution is no longer preserved. The temperature distribution is dependent on the shape of the column.

The results plotted in Fig. 4 can be collected in the array of temperature values $T_{kj}^{R*} \equiv T^{R*}(z_j, t_k)$. The star sign is here to underline that these reference temperatures are numerically generated, not measured in situ. This data array is used in the identification procedure to guess back the shape of the reference column.

4.2. Identification of column shape

For solving the optimization problem (2.2) differential evolution (DE) method is used. It belongs to the group of evolutionary algorithms such as genetic algorithms, genetic strategy, harmony search, swarm optimization, and many others. Its most important property, which was a key argument for using DE in this research is that this algorithm does not require any spatial differentiability of the fitness function [13, 17]. Differential evolution is a stochastic population-based method. At each pass through the population, the algorithm mutates each candidate solution by mixing it with other candidate solutions to create the next trial candidate. There are several strategies for creating trial candidates, which suit some problems more than others. In this research, the commonly used *best1bin* strategy is adopted. The main parameters that influence the optimization process and the final results within this strategy are the population size, which in this research is taken as 20 candidates, mutation constant (also known as differential weight) which is established adaptively during optimization from the range (0.5, 1) and the recombination constant (known also as crossover probability) set up to 0.7. The initial population of 20 candidates, i.e., initial candidate diameter vectors D_j are drawn randomly using the Latin hypercube method from the relatively broad diameter range, i.e., from 0.4 to 2.6 m. The same range was used during optimization for bounding the trial solutions.

Several runs of the optimization procedure, with different initial candidate populations, were executed to verify the reliability and convergence speed of the method. The maximum number of DE iterations is set up to 1000 and the convergence tolerance below 0.01 was required. Computations are performed on a server equipped with a 2x Intel Xeon Gold 5220R processor. For each optimization run 20 processor cores were used, so that trial I-BVPs were solved in parallel. Updates of the fitness function (defined by Eq. 2.2) for each run are shown in Fig. 5.

It is visible, that the algorithm achieves a fitness function value lower than 0.1 at every run. To realize that this is a particularly good result let us indicate that the average error in temperature fit is then certainly not greater than 0.025 K, which, in turn, translates to the average error in the identified column diameters not greater than, approximately, 2 m. This is considered as an insignificant shift in terms of engineering purposes. Every run of the optimization problem took a time between 1.5 to 3 hours, during which the fitness function is called from 75 000 to 150 000 times. This is a significant numerical effort. However,

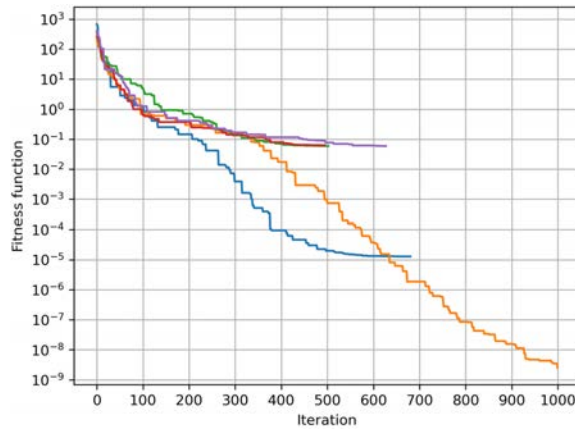


Fig. 5. Convergence of the differential evolution algorithm. 5 different runs were executed. The fitness function is defined by Eq. (2.2)

in engineering applications, this effort could be partially avoided by setting the realistic requirement on the final value of the fitness function.

5. Discussion of the results and conclusions

Identification results presented in the previous section are very promising and they are encouraging for further work. Preliminary computations performed also for other randomly generated reference columns show very similar results, i.e., very good shape identification is observed. However, when the depth resolution is increased the results are different. For example, if it is tried to identify the column shape at every 0.3 m (instead of 0.6 m) in depth, also using temperature measurements at every 0.3 m, optimization ends up with higher values of the fitness functions. Distinctly different column shapes are obtained with every run. Clearly in this case the temperatures observed at the centre of the column are not enough to identify its shape and more measurements must be done. However, it has to be underlined, that the *trends* in the column shapes seem to be still preserved, and the average diameter of the columns is always properly identified.

An important issue that has to be considered is the time needed for reliable shape identification. In this research temperature observations were limited to 72 hours. However, both shorter and longer times can be established. Shorter times are preferred since faster assessment of the quality of the jet-grouted column has an economic advantage and this will also speed up the optimization process (faster I-BVP solution). On the other hand, the longer times may add some important information to the fitness function, resulting in better identification results, but at the cost of longer computations. In general, to speed up the computations the differential evolution parameters could be manipulated, a coarser FE mesh can be tested or some advanced technics using surrogate models can be exploited,

as it is done in references [18, 19]. In this latest case, the optimization times can become negligible, but the effort is then moved to the preparation of a suitable surrogate model.

The influence of other model parameters on the solution, assumed here as given, also should be investigated. For example, the initial temperatures in the soil mass depend on the location and year season and this is of interest, how this is influencing the evolution of temperatures in the column. Similarly, one can ask what the sensitivity of the model on the variations of thermal conductivity coefficients is. Conductivity may vary in space and time (temperature). Another important issue is related to the assumed cement hydration model, which should reflect the heat production rate in the column as exactly as possible.

Finally, it has to be stated, that the method should be verified and calibrated on the real field data. Results described in [9, 10] show that gathering necessary temperature information from the freshly executed jet-grouted column is technologically possible and is recognized in geotechnical practice. Moreover, it seems that there are no technological obstacles for measuring the temperatures not only at the centre of the column but also at some distance from the trace of the injecting pipe, which might be advantageous for shape identification.

References

- [1] P. Croce, A. Flora, and G. Modoni, *Jet Grouting: technology, design and control*. London: CRC Press, 2014, doi: [10.1201/b16411](https://doi.org/10.1201/b16411).
- [2] P.G.A. Njock, J. Chen, G. Modoni, A. Arulrajah, and Y.-H. Kim, "A review of jet grouting practice and development", *Arabian Journal of Geosciences*, vol. 11, no. 16, 2018, doi: [10.1007/s12517-018-3809-7](https://doi.org/10.1007/s12517-018-3809-7).
- [3] D. Ribeiro and R. Cardoso, "A review on models for the prediction of the diameter of jet grouting columns", *European Journal of Environmental and Civil Engineering*, vol. 21, no. 6, pp. 641–669, 2017, doi: [10.1080/19648189.2016.1144538](https://doi.org/10.1080/19648189.2016.1144538).
- [4] T. Kimpritis, J.R. Standing, and R. Thurner, "Estimating column diameters in jet-grouting processes", *Proceedings of the Institution of Civil Engineers – Ground Improvement*, vol. 171, no. 3, pp. 148–158, 2018, doi: [10.1680/jgrim.17.00001](https://doi.org/10.1680/jgrim.17.00001).
- [5] J. Tinoco, A. Gomes Correia, and P. Cortez, "Jet grouting column diameter prediction based on a data-driven approach", *European Journal of Environmental and Civil Engineering*, vol. 22, no. 3, pp. 338–358, 2018, doi: [10.1080/19648189.2016.1194329](https://doi.org/10.1080/19648189.2016.1194329).
- [6] S.-L. Shen, P.G. Atangana Njock, A. Zhou, and H.-M. Lyu, "Dynamic prediction of jet grouted column diameter in soft soil using Bi-LSTM deep learning", *Acta Geotechnica*, vol. 16, no. 1, pp. 303–315, 2021, doi: [10.1007/s11440-020-01005-8](https://doi.org/10.1007/s11440-020-01005-8).
- [7] O.S. Langhorst, et al., "Design and validation of jet grouting for the Amsterdam Central Station", in *Geotechniek, Special Number on Madrid XIV European Conference of Soil Mechanics and Foundation Engineering*. 2007, pp. 20–23.
- [8] ASTM D5753-18 Standard Guide for Planning and Conducting Geotechnical Borehole Geophysical Logging. ASTM, 2018.
- [9] D. Adam, K. Meinhard, and R. Lackner, "Temperature measurements to determine the diameter of Jet-grouted columns", in *Proceedings of the DFI and EFFC 11th International Conference of Geotechnical Challenges in Urban Regeneration*. Eigenverlag, 2010.
- [10] K. Meinhard, "TEMPJET: continuous quality control and quality assurance", *World PORR*, vol. 160, 2012. [Online]. Available: <https://worldofporr.com/uploads/pdf/TEMPJETContinuousQualityControlandQualityAssurance.pdf>.

- [11] G.D. Byrne and A.C. Hindmarsh, “Polyalgorithm for the numerical solution of ordinary differential equations”, *ACM Transactions on Mathematical Software*, vol. 1, no. 1, pp. 71–96, 1975, doi: [10.1145/355626.355636](https://doi.org/10.1145/355626.355636).
- [12] L.F. Shampine and M.W. Reichelt, “The MATLAB ODE Suite”, *SIAM Journal on Scientific Computing*, vol. 18, no. 1, 1997, doi: [10.1137/S1064827594276424](https://doi.org/10.1137/S1064827594276424).
- [13] P. Virtanen, et al., “SciPy 1.0: fundamental algorithms for scientific computing in Python”, *Nature Methods*, vol. 17, no. 3, pp. 261–272, 2020, doi: [10.1038/s41592-019-0686-2](https://doi.org/10.1038/s41592-019-0686-2).
- [14] M. Wojciechowski, “Fempy – finite element method in python”, GitHub. [Online]. Available: <https://github.com/mrkwjw/fempy>; <http://fempy.org>. [Accessed 15 Mar. 2021].
- [15] C. Geuzaine and J.-F. Remacle, “Gmsh: A 3-D finite element mesh generator with built-in pre- and post-processing facilities”, *International Journal for Numerical Methods in Engineering*, vol. 79, no. 11, pp. 1309–1331, 2009, doi: [10.1002/nme.2579](https://doi.org/10.1002/nme.2579).
- [16] T.A. Davis, “Algorithm 832: UMFPACK V4.3—an unsymmetric-pattern multifrontal method”, *ACM Transactions on Mathematical Software*, vol. 30, no. 2, pp. 196–199, 2004, doi: [10.1145/992200.992206](https://doi.org/10.1145/992200.992206).
- [17] R. Storn and K. Price, “Differential evolution – a simple and efficient heuristic for global optimization over continuous spaces”, *Journal of Global Optimization*, vol. 11, no. 4, pp. 341–359, 1997, doi: [10.1023/A:1008202821328](https://doi.org/10.1023/A:1008202821328).
- [18] M. Wojciechowski, “Application of artificial neural network in soil parameter identification for deep excavation numerical model”, *Computer Assisted Methods in Engineering and Science*, vol. 18, no. 4, art. no. 4, 2017. [Online]. Available: <https://cames.ippt.pan.pl/index.php/cames/article/view/109>.
- [19] M. Wojciechowski, M. Lefik, and D. Boso, “Inverse problems in the light of homogenisation methods: identification of a composite microstructure”, *International Journal for Multiscale Computational Engineering*, vol. 20, no. 5, pp. 33–51, 2022, doi: [10.1615/IntJMultCompEng.2022040213](https://doi.org/10.1615/IntJMultCompEng.2022040213).
- [20] L. Wanik, J. Bzówka, and G. Modoni, “Influence of technological parameters on the properties of jet grouting columns detected with full scale experiments”, *Archives of Civil Engineering*, vol. 69, no 2, pp. 417–433, 2023, doi: [10.24425/ace.2023.145276](https://doi.org/10.24425/ace.2023.145276).

Identyfikacja kształtu kolumny jet-grouting na podstawie analizy termicznej i ewolucji różnicowej

Słowa kluczowe: hydratacja cementu, iniekcja strumieniowa, kolumna jet-grouting, niustalony przepływ ciepła, problem odwrotny

Streszczenie:

W artykule przedstawiono metodę identyfikacji kształtu świeżo wykonanej kolumny typu jet-grouting. Metoda polega na wstecznej analizie temperatur mierzonych wewnątrz kolumny, wzdłuż śladu żerdzi iniekcyjnej. Zmiany temperatur w kolumnie są wynikiem hydratacji zaczynu cementowego. W celu określenia kształtu kolumny, który najlepiej pasuje do referencyjnych pomiarów temperatur, wykorzystano globalny algorytm optymalizacyjny zwany ewolucją różnicową. W ramach tego algorytmu formułowano próbne problemy początkowo-brzegowe, w postaci dwuwymiarowego, osiowo-symetrycznego zagadnienia niustalonego przewodzenia ciepła, które rozwiązywano za pomocą metody elementów skończonych. Wykazano, że proponowana metoda pozwala na dokładne odwzorowanie kształtu kolumny, jeśli tylko model numeryczny poprawnie odwzorowuje rzeczywistość fizyczną. Zaletą metody w porównaniu do wcześniejszych rezultatów jest możliwość identyfikacji zmian średnicy kolumny wzdłuż jej długości, a nie tylko identyfikacja pojedynczej średnicy przy założonym kształcie walcowym kolumny.

Received: 2023-07-25, Revised: 2023-08-08